




Multifunctional ultralight nanocellulose aerogels as excellent broadband acoustic absorption materials

Ju-Qi Ruan^{1,*} , Kai-Yue Xie¹, Zhaoxi Li², Xiaoqing Zuo³, Wei Guo¹, Qing-Yuan Chen¹, Houyin Li¹, Chunlong Fei^{2,*}, and Ming-Hui Lu⁴

¹School of Physics Science and Technology, Kunming University, Kunming 650214, China

²School of Microelectronics, Xidian University, Xi'an 710126, China

³Faculty of Materials Science and Engineering, Kunming University of Science and Technology, Kunming 650093, China

⁴National Laboratory of Solid State Microstructures, Nanjing University, Nanjing 210093, China

Received: 23 November 2022

Accepted: 21 December 2022

Published online:

1 January 2023

© The Author(s), under exclusive licence to Springer Science+Business Media, LLC, part of Springer Nature 2022

ABSTRACT

Noise pollution has become one of the environmental hazards in parallel with air pollution, water pollution, and solid waste pollution worldwide. Cellulose aerogel is a new porous sound-absorbing material that is highly efficient, green, recyclable, and degradable, showing bright prospect for the application in noise suppression. In this study, we fabricated multifunctional acoustic absorptive cellulose nanocrystal (CNC) aerogels by employing calcium chloride as the green crosslinker of CNC, followed by freeze drying. The as-prepared CNC aerogels exhibit excellent broadband acoustic absorption performance with a high maximum absorption coefficient of 0.99 (at 2960 Hz), an average absorption coefficient of 0.85 (in the range of 600–6400 Hz), and a wide absorption bandwidth of 4673 Hz with the absorption coefficient greater than 0.8. The dissipation mechanism of sound energy in the fabricated CNC aerogels is predicted by a designed porous media model. Moreover, good thermal stability, ultralight property (density of 0.036 g/cm³), and high diffuse reflection characteristics (average diffuse reflectance of 98.17% for light) of these CNC aerogels were demonstrated as well. Such versatile aerogel materials not only pave the way for the development of sustainable and efficient acoustic absorption materials, but also have great potential applications in broad fields including construction, transportation, and environment acoustics.

Handling Editor: Stephen Eichhorn.

Address correspondence to E-mail: ruanjuqi@foxmail.com; clfei@xidian.edu.cn

<https://doi.org/10.1007/s10853-022-08118-3>

Introduction

Noise is known as an “invisible killer,” which seriously threatens human health and quality of life worldwide [1]. As an effective medium to eliminate noise, porous sound-absorbing materials play a prominent role in wide fields, e.g., acoustical engineering, architectural insulation, rail transit, and high-end equipment manufacturing [2–5]. However, the commonly used porous sound-absorbing materials (wood fiber, polyester fiber, and mineral wool) generally lack comprehensive properties including environmental friendliness, safety, and functionality. Therefore, it is urgent to develop new highly efficient acoustic absorption materials with multiple functions for advanced applications.

As a newly born third-generation aerogel material, cellulose aerogels not only inherit the advantages of cellulose including wide source, environmental friendliness, and sustainability [6], but also provide superior adjustable porous structure, e.g., super-high open porosity (up to 98.4%) [7], ultralow bulk density (as low as 0.047 g/cm^3) [8], extremely large specific surface area ($356 \text{ m}^2/\text{g}$), and pore volume ($1.27 \text{ cm}^3/\text{g}$) [9], which give them strong competitive advantages for the application in noise suppression. Since early reports on the acoustic absorption capability of ligno-cellulose aerogels (achieving an absorption coefficient of 0.827 at 1000 Hz with thickness of 15 mm) fabricated with ionic liquid (1-allyl-3-methylimidazolium chloride) [10], there has been an upsurge in researches on noise control of cellulose aerogels. Among them, acoustic absorptive cellulose aerogels prepared with polyvinyl alcohol (PVA) as the crosslinker are most concerned [11–13]. Dora et al. [14] synthesized a flexible macroscopic cellulose aerogel (SBA) based on sugarcane bagasse cross-linked with PVA. The as-prepared SBA (10 mm thick) exhibits excellent acoustic absorption performance with a maximum absorption coefficient (A_{\max}) above 0.9 around 3600 Hz, and a high average absorption coefficient (A_{ave}) of 0.861 between 1300 and 2500 Hz. Besides PVA, epichlorohydrin [15] or N, N'-methylene bisacrylamide [16] is also a well-qualified cross-linking agent to form cellulose aerogels with high acoustic absorption capability. Meanwhile, cellulose aerogels constructed with gelatin and their corresponding noise reduction effect have also been widely investigated [17]. A typical study is that Shan et al. [18] developed a cellulose-based aerogel (SLB-G)

derived from waste bamboo fibers and gelatin. The SLB-G (12 mm thick) possesses a competent noise reduction ability with a high sound transmission loss above 30 dB around 500 Hz. Recently, a class of novel bacteria-based cellulose aerogels (BCA) was developed and applied to the study of acoustic absorption [19]. The BCA reveals superior acoustic absorption abilities at broad frequencies from 200 to 6000 Hz with an A_{\max} of 0.97 located at 1500 Hz [20]. However, due to the single function of cellulose aerogels themselves, various optimization methods such as sulfuric acid hydrolysis [21] and methyltrimethoxysilane modification [22] were employed to enhance their thermal insulation and hydrophobicity so as to expand their practicality.

The successful creation of composite cellulose aerogels greatly enriches the functionality of cellulose aerogel materials with high mechanical strength, flame retardancy, temperature resistance, etc., thus further broadening their application prospect in the field of noise management [23–25]. Lin et al. [26] selected rod-shaped cellulose extracted from pineapple shell as the scaffold and combined it with iron-containing red mud to fabricate an organic–inorganic hybrid aerogel. The maximum absorption coefficient (A_{\max}) of a 10-mm-thick sample can reach 0.787 at 6000 Hz, which is higher than that of wood-based sound-absorbing panels such as fiberboard, particleboard, and plywood. Similarly, the silica/cellulose compound aerogels also show strong competitiveness in terms of acoustic insulation [27, 28]. Silviana et al. [29] explored the combination of newspaper waste-derived cellulose and silica from geothermal solid waste to produce a Si–cellulose aerogel as an enhanced sound insulation composite material, which, as the results show, has an A_{\max} of 0.999 when the mass fraction of the cellulose reaches 25%. Moreover, a series of cellulose-embedded aerogel composites are also quite representative [30]. This kind of material usually possesses hierarchical pore structure and can achieve unique acoustic absorption (A_{\max} above 0.9 in the range of 3500–6400 Hz, and a noise reduction coefficient of 0.45) with the thickness of about 20 mm [31]. In addition, a novel hierarchically maze-like structured aerogel compounded with polyacrylonitrile and cellulose nanofibers attracts much attention because it can achieve efficient acoustic absorption in a relatively low-frequency range [32].

The above-mentioned researches are representatives which strongly confirmed the application

potential of cellulose aerogels as a new type of green functional sound-absorbing material. Nevertheless, the acoustic absorption properties of cellulose aerogels, especially their absorption efficiency and bandwidth, are a subject to be further improved for wider applications. In this study, we fabricated the multifunctional acoustic absorptive cellulose nanocrystal (CNC) aerogels through a straightforward method by employing calcium chloride as the green crosslinker [33–36], followed by freeze drying. The influential mechanism of the porous structure on the acoustic absorption performance of the obtained CNC aerogels was investigated through the experiment combined with a designed porous media model. The results demonstrated their excellent broadband acoustic absorption performance as well as multifunctionality, revealing them as a promising material for the application in the field of noise reduction.

Experimental section

Materials

Cellulose nanocrystal (CNC) was provided by ScienceK New Material Technology Co., Ltd. (Soochow, China). Calcium chloride anhydrous (CaCl_2 , $\geq 96\%$) and tert-butyl alcohol ($\geq 99\%$) were purchased from Xilong Scientific Co., Ltd. (Swatow, China). All chemical reagents are of analytical grade and used as-received without further purification. Deionized water ($\text{DI}\cdot\text{H}_2\text{O}$) is of laboratory grade and used throughout the experiment.

Preparation of the CNC aerogels

The preparation process of the CNC aerogels in this study is shown in Fig. 1. First, 0.5 g CNC was dissolved in 99.5 ml $\text{DI}\cdot\text{H}_2\text{O}$ by mechanically stirring at

300 rpm for 1 h at room temperature, followed by thoroughly dispersing through an ultrasonic equipment (JP-100PLUS) with the power of 1000 W for 20 min to obtain a viscous transparent CNC dispersion. Later, 30 ml CaCl_2 solution with concentration of 0.05 mol/L was added to the above dispersion drop by drop to cross-link CNC, which led to the production of the homogeneous CNC suspension. Subsequently, the CNC suspension was centrifuged by a high-speed centrifuge (JIDI-16D) for 5 min with the speed of 10,000 rpm and then poured into a set mold and solidified for 8 h to form the CNC hydrogel. During the period of solidification, the bubbles were vacuumed out, if any, from the structure of the pregenerated CNC hydrogel via a vacuum pumping device. Then, the CNC hydrogel was soaked in $\text{DI}\cdot\text{H}_2\text{O}$ to remove residual chemical reagents until the pH value of the soaking solution reaches 7 to get the swelling equilibrium of the CNC hydrogel [16]. Afterward, the CNC hydrogel was aged in proper aging solvent at $50\text{ }^\circ\text{C}$ for 3 days, during which the aging solvent was exchanged every 12 h. Finally, the hydrogel was frozen by using liquid nitrogen as the medium at $-196\text{ }^\circ\text{C}$ for 30 min and then placed in a vacuum freeze drier to dry for 48 h (NAI-L4-80D, at $-80\text{ }^\circ\text{C}$ with the vacuum pressure below 10 Pa) to obtain the CNC aerogel. Here, three types of aging solvent, i.e. tert-butyl alcohol, the mixture of tert-butyl alcohol and $\text{DI}\cdot\text{H}_2\text{O}$ (volume ratio of 1:1), and $\text{DI}\cdot\text{H}_2\text{O}$, were employed to soak the CNC hydrogel in the aging process. The corresponding obtained CNC aerogels are named as CNCA-t, CNCA-m, and CNCA-h, respectively.

Characterizations

The macroscopic appearance of the CNC aerogels was observed through visual examination. The morphology of them was examined using the micrograph

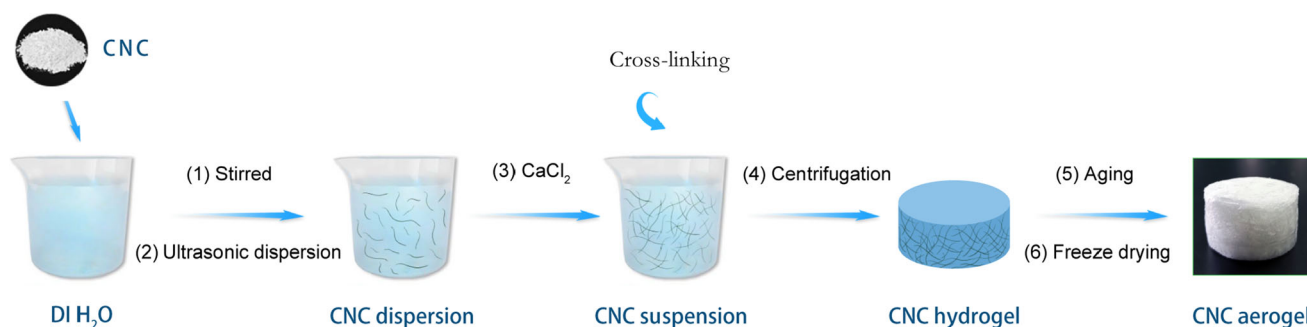


Figure 1 Schematic illustration of the preparation process of the cellulose nanocrystal (CNC) aerogels.

obtained from a scanning electron microscope (SEM, Hitachi S-3400 N, Japan). The accelerating voltage was 15 kV, and all the specimens were sprayed with platinum in advance. The characteristics of the porous structure of the CNC aerogels, including average aperture, most probable aperture, and porosity, were measured and analyzed using a mercury porosimetry analyzer (Micromeritics AutoPore Iv 9510, America) with the recognizable aperture ranging from 5 nm to 800 μm . The porosity of the CNC aerogels is able to be estimated by the following formula:

$$\text{Porosity}(\%) = 1 - \frac{\rho_b}{\rho_s} \times 100\% \quad (1)$$

where ρ_b indicates the bulk density of the CNC aerogels, which can be obtained from the mercury porosimetry measurement. And ρ_s represents the skeleton density of the aerogels, and its theoretical value can be considered as 1.528 g/cm^3 [37–39].

The chemical structures of the CNC aerogels were explored by a Fourier-transform infrared (FT-IR) spectra spectrophotometer (Bruker Tensor 27, Germany) in the range of 4000–400 cm^{-1} with a resolution of 1.92 cm^{-1} . The thermal stability of the CNC aerogels was mainly tested by thermogravimetry (Netzsch TG 209 F1 Libra, Germany), and the sample was heated from 50 to 800 $^{\circ}\text{C}$ at a heating rate of 10 K/min in nitrogen atmosphere. Acoustic absorption performance of the CNC aerogels was evaluated by the normal acoustic absorption coefficient, which was measured using a B&K type 4206 impedance tube based on a two-microphone transfer function method in accordance with the ASTM E1050 standard (Fig. S1 of the supplementary information). The measurement range of sound-absorbing frequency is 600–6400 Hz, and the thickness of the sample is 15 mm. The diffuse reflectance of the specimens was measured using a spectrophotometer (Shimadzu UV-3600i Plus, Japan), covering the visible light wavelength range of 400–800 nm.

Results and discussion

Characteristics of the porous structure of the CNC aerogels

Figure 2a, b and c shows the optical photographs of the fabricated CNC aerogels. Because the sublimation of ice crystals accompanying the freeze-drying

process can effectively avoid the damage of liquid capillary force to the porous networks of cellulose, all the aerogel samples maintain high morphology integrity without cracks [11]. The aging solvents have a significant effect on the contraction rate of the CNC aerogels. An obvious shrinkage occurred on the CNC aerogel that used tert-butyl alcohol as the aging solvent (Fig. 2a). Such structural contraction can be effectively mitigated by adding an appropriate amount of DI-H₂O into the tert-butyl alcohol aging solvent (Fig. 2b) and even be almost completely avoided by employing pure DI-H₂O as the aging solvent, which also results in the smooth appearance of CNCA-h (Fig. 2c). This is due to the fact that compared with tert-butyl alcohol, the higher volume expansibility of ice crystals under snap freezing conditions can lead to the formation of fluffier porous structure for CNC aerogels. Further, the effect of the aging solvents on the porous structure of the CNC aerogels can be intuitively reflected by SEM images. As shown in Fig. 2d and e, both CNCA-t and CNCA-m show unobvious porous characteristics at the low magnification and present a dense reticular structure when the magnification increases (Fig. 2d' and e'). And yet, CNCA-h exhibits excellent loose porous structure with obvious larger pores (Fig. 2f and f') compared to CNCA-t and CNCA-m. The formation of such fluffy network for CNCA-h was attributed to the rapid expansion of ice crystals in the freezing procedure; the growing ice crystals rejected the CNC skeleton, and the CNC network with larger pores was formed between the boundaries of neighboring ice crystals [32]. The optimization effect of DI H₂O on the porous characteristics of the CNC aerogels can be further quantitatively confirmed in Table 1. Compared with CNCA-t, change in the structural parameters of CNCA-m is not evident. This is principally because to a certain degree, tert-butyl alcohol inhibited the rapid growth of ice crystals. However, as the volume expansibility of ice crystals is much higher than that of tert-butyl alcohol under freezing, by employing DI H₂O as the aging solvent, CNCA-h can finally form fluffier porous structure to ensure that acoustic waves easier to enter the overall structure. Evidently, compared to CNCA-t (Table 1), CNCA-h possesses unique porous features with the increased average aperture from 0.19 to 0.45 μm , most probable aperture (Fig. S2 of the supplementary information) from 14.91 to 96.19 μm , porosity from 94.29 to 97.62%, and permeability from 0.32 to 50.03

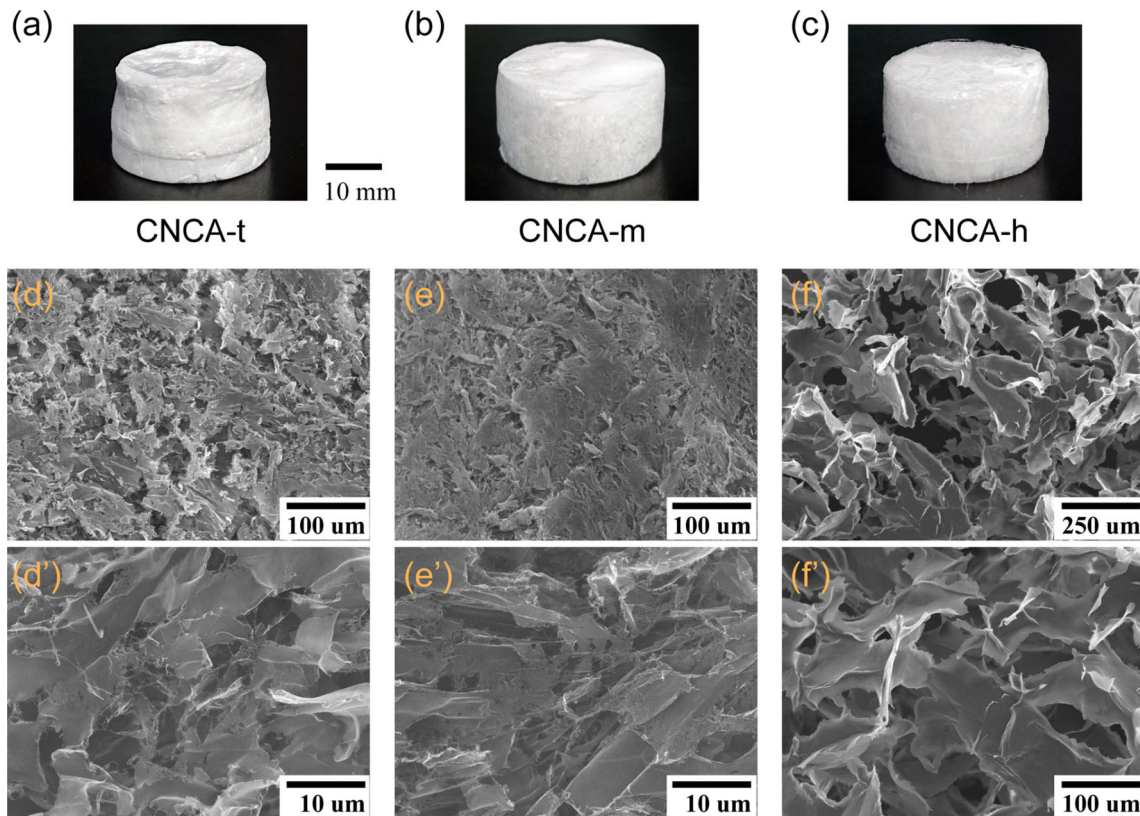


Figure 2 Optical photographs a–c and SEM images of as-prepared CNC aerogels. d and d', e and e', f and f' show the morphology of CNCA-t, CNCA-m, and CNCA-h at low and high magnification, respectively.

Table 1 Porous structure parameters of the CNC aerogels

	Average aperture (μm)	Most probable aperture (μm)	Permeability (Darcy)	Porosity (%)
CNCA-t	0.19	14.91	0.32	94.29
CNCA-m	0.19	14.90	19.54	95.07
CNCA-h	0.45	96.19	50.03	97.62

Darcy. Here, the permeability refers to how easy the material allows mercury vapor to pass through. In a certain extent, it can reflect the fluffiness of the CNC aerogels' structure. As a result, DI- H_2O plays an important role in promoting an excellent permeable porous structure for CNC aerogels, endowing them with higher efficiency to permeate and dissipate sound energy.

Physical and chemical properties of the CNC aerogels

Figure 3 investigates the fabricated CNC aerogels' physical properties focusing on the bulk density. As shown in Fig. 3a, these CNC aerogels possess significantly lower density compared with several

typical porous sound-absorbing materials. As the high volume expansibility of ice crystals can generate considerable voids in the porous networks of cellulose and then make it looser from the inside, the density of the obtained CNC aerogels decreases with the increase in water content of the aging solvents. Notably, a block of CNCA-h can stand stably on a dandelion, while the fluff of the dandelion is not affected (Fig. 3b), which demonstrates the ultralightness characteristic of CNCA-h (density of 0.036 g/cm^3). Such ultralow density is very conducive to enhancing the acoustic impedance matching at the aerogel–air interface [40].

To further investigate the CNC aerogels' chemical structure, the Fourier-transform infrared (FT-IR)

Figure 3 **a** Bulk density of the fabricated CNC aerogels compared with the commonly used porous sound-absorbing materials. **b** CNC aerogel standing on a dandelion.

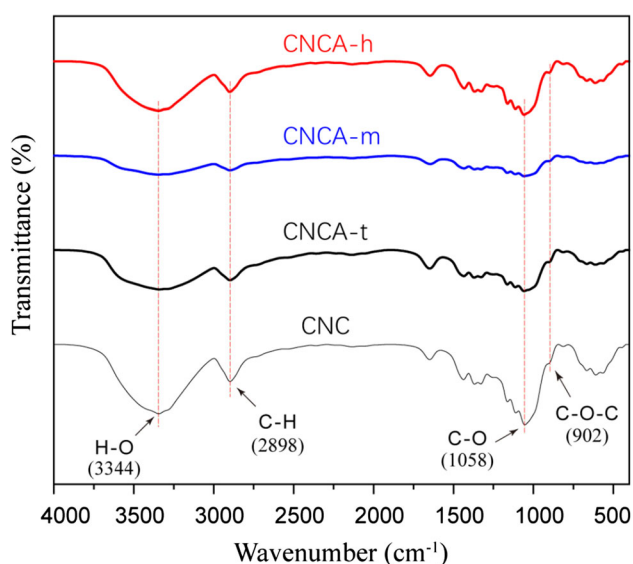
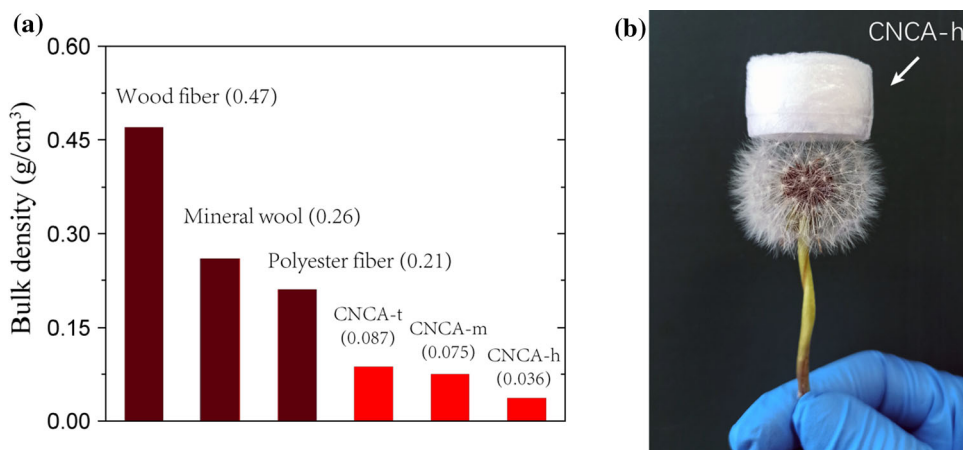


Figure 4 Fourier-transform infrared (FT-IR) spectra of the fabricated CNC aerogels compared with raw cellulose nanocrystal (CNC).

spectroscopy data were collected (Fig. 4). It can be seen that all the CNC aerogels show characteristic absorption bands at 3344, 2898, and 1058 cm⁻¹, corresponding to the H–O bond stretching vibration, C–H bond stretching vibration, and C–O bond valence vibration, respectively. These are the typical characteristic peaks of cellulose molecules, which suggest that the main components of CNC still existed after dissolution [16]. Meanwhile, the peak formed at 902 cm⁻¹ was probably caused by the stretching vibration of $\beta(1 \rightarrow 4)$ -glycosidic bond (C–O–C), which indicates that the cellulose chain was not broken during the chemical cross-linking process. Compared with CNC, the distinct shrinkage of peak

at 3344 cm⁻¹ for the fabricated CNC aerogels is attributed to the notable loss of inter- and intra-hydrogen bonds caused by metal (Ca²⁺) addition, validating the involvement of CaCl₂ in the chemical cross-linking of the cellulose hydrogel [35]. In addition, the CNC aerogels were tested by thermogravimetric (TG) analysis to evaluate their thermal stability. As shown in Fig. 5a, the pyrolysis process of the CNC aerogels goes through four main stages: (I) initial pyrolysis (50–100 °C), (II) stability at low temperatures (100–200 °C), (III) rapid pyrolysis (200–400 °C), and (IV) stability at high temperatures (400–800 °C). In stage (I), all the aerogel samples experienced a slight weight loss about 5%, which was mainly caused by the evaporation of free water captured by the hydroxyl groups of cellulose chain from the air. After that, the quality of the samples tends to be stable during stage (II). When the temperature continues to increase in stage (III), all the CNC aerogels undergo severe pyrolysis with considerable weight loss, which is mainly related to the thermal oxidative decomposition of cellulose [41]. Except for the pyrolysis of cellulose, the pyrolysis process of CNCA-t and CNCA-m is accompanied by the decomposition of the compounds produced by the complex reaction between tert-butyl alcohol and CaCl₂. Hence, CNCA-t and CNCA-m exhibit greater weight loss (75.30–77.32%) compared to CNCA-h (63.10%). When the temperature rises above 400 °C, the water in each sample is basically lost, causing the TG curve to flat gradually. Furthermore, it can be seen from the DTG curves (Fig. 5b) that CNCA-h presents a relatively lower maximum loss rate (8.77%/min) compared with CNCA-t and CNCA-m (10.58–12.72%/min, respectively), demonstrating

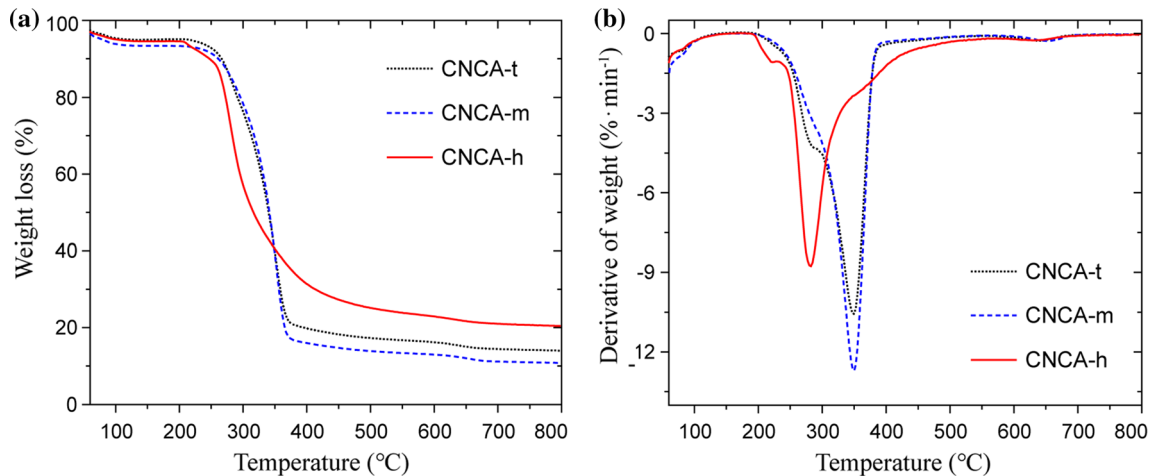


Figure 5 Thermogravimetric (TG) curve (a) and differential thermogravimetric (DTG) curve (b) of the CNC aerogels.

better thermal stability. It can be concluded that CNCA-h has the maximum working temperature between 200 and 282 °C, showing good potential for application in relatively high-temperature environments.

Acoustic absorption performance of the CNC aerogels

Figure 6a shows the normal incident acoustic absorption coefficient as a function of the frequency for the CNC aerogels. Strikingly, CNCA-h presents a greater acoustic absorption coefficient than CNCA-t and CNCA-m over the entire frequency domain, which, in brief, can be explained from two aspects: reduction of sound reflection and enhancement of sound dissipation [42]. On the one hand, compared with CNCA-t and CNCA-m, the significantly decreased density of CNCA-h (0.036 g/cm³) is closer to the density of air. This will lead to a lower characteristic acoustic impedance for CNCA-h, which is very helpful in strengthening the impedance matching at the structure–air interface and effectively reducing the reflection of acoustic waves [40]. Meanwhile, the fluffier structure of CNCA-h (with obvious higher permeability and larger pore size, Table 1 and Fig. 2) is easier to let the vibrating air molecules, e.g., O₂ and N₂, to penetrate deep enough to the material [43]. This is beneficial for ensuring that acoustic waves with a wide frequency range enter the overall structure of CNCA-h. On the other hand, CNCA-h possesses higher porosity (Table 1)

compared to CNCA-t and CNCA-m. This will result in a greatly expanded microstructured air–solid interfacial area for CNCA-h. During the incidence of an airborne sound, such enlarged interfacial area will provide more efficient viscous and thermal losses to sound energy and can simultaneously enhance the multiple reflections of the acoustic wave to extend its propagation path inside the structure of CNCA-h [40, 44]. Therefore, the acoustic absorption coefficient of CNCA-h is significantly higher compared with that of CNCA-t and CNCA-m. Similarly, the slight improvement in acoustic absorption of CNCA-m relative to CNCA-t can also be explained. Table 2 summarizes the acoustic absorption properties of these CNC aerogels. Bandwidth (BW) refers to the number of frequency points with an acoustic absorption coefficient greater than 0.8, and it is employed here to evaluate the broadband acoustic absorption behavior of the CNC aerogels. Notably, CNCA-h exhibits significantly higher BW (4673 Hz), A_{ave} (0.85), as well as A_{max} (0.99) compared with CNCA-t and CNCA-m, showing efficient and broadband acoustic absorption characteristics.

In addition, in order to verify the dissipation mechanism of sound energy in the structure of the CNC aerogels, COMSOL Multiphysics was used to develop numerical simulation of the porous structure combining finite element method with a three-parameter analytical model [45, 46]. In this model, the surface acoustic impedance of porous media can be predicted by determining its three non-acoustic parameters: porosity, average aperture, and standard

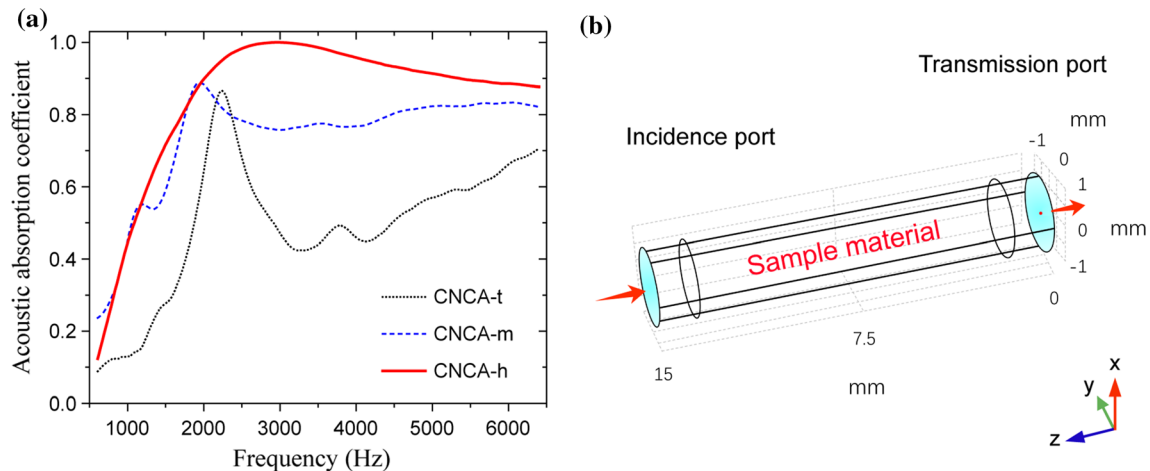


Figure 6 **a** Normal acoustic absorption coefficient as a function of frequency for the CNC aerogels. **b** Schematic of the designed porous media model to predict the acoustic absorption behavior.

Table 2 Acoustic absorption properties of the CNC aerogels

	Average absorption coefficient A_{ave}	Maximum absorption coefficient A_{max}	Bandwidth BW (Hz)
CNCA-t	0.49	0.87	225
CNCA-m	0.74	0.89	2514
CNCA-h	0.85	0.99	4673

deviation of aperture. Then, the normal acoustic absorption coefficient can be calculated [46]. Here, according to the pore characteristics of fabricated CNC aerogels (Fig. S2 of the supplementary information), the average aperture is instead by the most probable aperture to adjust the model. As shown in Fig. 6b, the CNC aerogel is set up as a cylinder wave guide with the related structural parameters in Table 1. The acoustic wave is incident from one port on the bottom surface of the cylinder, and its transmission at the other port is observed. Then, the acoustic absorption coefficient A can be calculated using the following equation:

$$A = 1 - |R|^2 - |T|^2 \quad (2)$$

where R and T are the reflection and transmission coefficients obtained from the two ports, respectively. The acoustic absorption coefficient was predicted through a frequency sweeping from 600–6400 Hz (Figs. S3 and S4 of the supplementary information). The results, to some extent, can predict the acoustic absorption behavior including the A_{ave} (0.87) and BW (4800 Hz) for CNCA-h, as well as the increasing trend of acoustic absorption coefficient among the fabricated CNC aerogels.

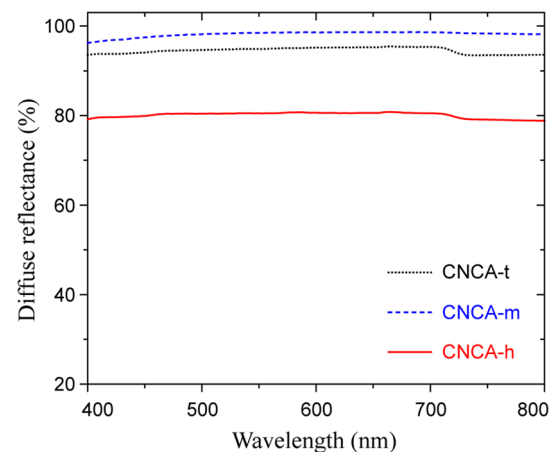
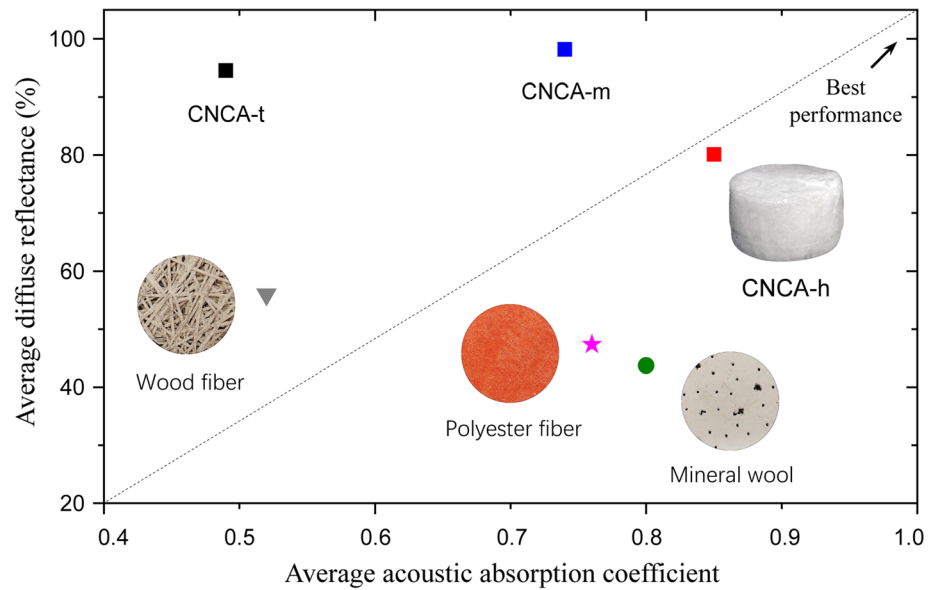


Figure 7 Diffuse reflection behavior of the CNC aerogels in visible light band.

Comprehensive performance of the CNC aerogels

Figure 7 shows the optical performance represented by the diffuse reflection of the CNC aerogels. All the aerogel samples exhibit superior broadband diffuse reflection characteristics across the visible light. Such unique optical behavior mainly results from the dense nanosized scattering centers on the surface of

Figure 8 An experimental map to compare the comprehensive performance of acoustics and optics between the fabricated CNC aerogels as well as several typical porous sound-absorbing materials.



the CNC aerogels, which hence give them a white appearance [47, 48]. As the fluffier structure of CNCA-h (larger pores and higher porosity) allows light waves to pass through more easily, its average diffuse reflectance (80.11%) decreases slightly compared with CNCA-t (94.51%) and CNCA-m (98.17%). Nevertheless, CNCA-h still provides superior diffuse reflective performance compared with the commonly used sound-absorbing materials.

Ultimately, we summarize an experimental map (Fig. 8) to comparatively analyze the comprehensive performance of acoustics and optics between the CNC aerogels and several traditional porous sound-absorbing materials. Inside, the acoustic absorption ability is expressed as the average acoustic absorption coefficient, and the optical performance is symbolized by the average diffuse reflectance. Evidently, CNCA-h locates in the upper right corner of the map, exhibiting the best overall performance for acoustics and optics. These results demonstrate fine multifunctionality of CNCA-h, endowing it with good prospect to be an advantageous acoustic absorption material.

Conclusions

We fabricated the CNC aerogels through a straightforward method by employing calcium chloride as the green crosslinker, followed by freeze drying. Deionized water plays an important role as the aging solvent to produce superior porous characteristics to

dissipate sound energy, e.g., the larger pore size, higher porosity, and ultralow density for the CNC aerogels. Hence, excellent broadband acoustic absorption performance is produced. Follow-up research will focus on exploring the mechanical properties, as well as the internal relationship between structural control and acoustic absorption properties to deeply clarify the dissipation mechanism of sound energy in the structure of the CNC aerogels. Characterized by such advantages as ultralightness, good thermal stability, and high diffuse reflection for light, the CNC aerogels can be used as a promising green multifunctional sound-absorbing material for various applications.

Acknowledgements

This work was supported by the Yunnan Fundamental Research Projects (Grant Nos. 202201AU070036, 202101BA070001-175, and 202101BA070001-162), the National Natural Science Foundation of China (Grant Nos. 52261009 and 12165010), the Science Foundation of the National Laboratory of Solid State Microstructures, the Science Foundation of Kunming University (Grant No. YJL20014), the Key Laboratory of Artificial Microstructures in Yunnan Higher Education Institutions, the Program for Innovative Research Team in Kunming University, and the Cooperation Program of XDU-Chongqing IC Innovation Research Institute (Grant No. CQIRI-2022CXY-Z07).

Author contributions

JQR and QYC contributed to conceptualization and design; all authors were involved in data curation and formal analysis; investigation and methodology; and manuscript writing and editing; JQR, WG, and XZ contributed to funding acquisition; and JQR, CF, and MHL were involved in project administration and supervision.

Data availability

The data that support the findings of this study are available from the corresponding authors upon reasonable request.

Declarations

Conflict of interest The authors declare that they have no conflict of interest.

Supplementary Information: The online version contains supplementary material available at <http://doi.org/10.1007/s10853-022-08118-3>.

References

- [1] Thompson R, Smith RB, Karim YB, Shen C, Drummond K, Teng C, Toledano MB (2022) Noise pollution and human cognition: An updated systematic review and meta-analysis of recent evidence. *Environ Int* 158:106905. <https://doi.org/10.1016/j.envint.2021.106905>
- [2] Strobach E, Bhatia B, Yang S, Zhao L, Wang EN (2019) High temperature stability of transparent silica aerogels for solar thermal applications. *APL Mater* 7:081104. <https://doi.org/10.1063/1.5109433>
- [3] Lázaro J, Pereira M, Costa PA, Godinho L (2022) Performance of low-height railway noise barriers with porous materials. *Appl Sci* 12:2960. <https://doi.org/10.3390/app12062960>
- [4] Tao Y, Ren M, Zhang H, Peijs T (2021) Recent progress in acoustic materials and noise control strategies: a review. *Appl Mater Today* 24:101141. <https://doi.org/10.1016/j.apmt.2021.101141>
- [5] Cao L, Fu Q, Si Y, Ding B, Yu J (2018) Porous materials for sound absorption. *Compos Commun* 10:25–35. <https://doi.org/10.1016/j.coco.2018.05.001>
- [6] Zimmermann T, Bordeanu N, Strub E (2010) Properties of nanofibrillated cellulose from different raw materials and its reinforcement potential. *Carbohydr Polym* 79:1086–1093. <https://doi.org/10.1016/j.carbpol.2009.10.045>
- [7] Wang M, Anoshkin IV, Nasibulin AG, Korhonen JT, Seitsonen J, Pere J, Kauppinen EI, Ras RHA, Ikkala O (2013) Modifying native nanocellulose aerogels with carbon nanotubes for mechanoresponsive conductivity and pressure sensing. *Adv Mater* 25:2428–2432. <https://doi.org/10.1002/adma.201300256>
- [8] Zhao Y, Zhong K, Liu W, Cui S, Zhong Y, Jiang S (2020) Preparation and oil adsorption properties of hydrophobic microcrystalline cellulose aerogel. *Cellulose* 27:7663–7675. <https://doi.org/10.1007/s10570-020-03309-0>
- [9] Cai J, Liu S, Feng J, Kimura S, Wada M, Kuga S, Zhang L (2012) Cellulose–silica nanocomposite aerogels by in situ formation of silica in cellulose gel. *Angew Chem Int Ed* 51:2076–2079. <https://doi.org/10.1002/ange.201105730>
- [10] Lu Y, Sun Q, Yang D, She X, Yao X, Zhu G, Liu Y, Zhao H, Li J (2012) Fabrication of mesoporous lignocellulose aerogels from wood via cyclic liquid nitrogen freezing–thawing in ionic liquid solution. *J Mater Chem* 22:13548–13557. <https://doi.org/10.1039/C2JM31310C>
- [11] Thai QB, Chong RO, Nguyen PTT, Le DK, Le PK, Phan-Thien N, Duong HM (2020) Recycling of waste tire fibers into advanced aerogels for thermal insulation and sound absorption applications. *J Environ Chem Eng* 8:104279. <https://doi.org/10.1016/j.jece.2020.104279>
- [12] Do NHN, Luu TP, Thai QB, Le DK, Chau NDQ, Nguyen ST, Le PK, Phan-Thien N, Duong HM (2020) Heat and sound insulation applications of pineapple aerogels from pineapple waste. *Mater Chem Phys* 242:122267. <https://doi.org/10.1016/j.matchemphys.2019.122267>
- [13] Tran DT, Nguyen ST, Do ND, Thai NTN, Thai QB, Huynh HKP, Nguyen VTT, Phan AN (2020) Green aerogels from rice straw for thermal, acoustic insulation and oil spill cleaning applications. *Mater Chem Phys* 253:123363. <https://doi.org/10.1016/j.matchemphys.2020.123363>
- [14] Kumar G, Dora DTK, Jadav D, Naudiyal A, Singh A, Roy T (2021) Utilization and regeneration of waste sugarcane bagasse as a novel robust aerogel as an effective thermal, acoustic insulator, and oil adsorbent. *J Clean Prod* 298:126744. <https://doi.org/10.1016/j.jclepro.2021.126744>
- [15] Moosavi S, Gan S, Chia CH, Zakaria S (2020) Evaluation of crosslinking effect on thermo-mechanical, acoustic insulation and water absorption performance of biomass-derived cellulose cryogels. *J Polym Environ* 28:1180–1189. <https://doi.org/10.1007/s10924-020-01676-0>
- [16] Lou CW, Zhou X, Liao X, Peng H, Ren H, Li TT, Lin JH (2021) Sustainable cellulose-based aerogels fabricated by directional freeze-drying as excellent sound-absorption

- materials. *J Mater Sci* 56:18762–18774. <https://doi.org/10.1007/s10853-021-06498-6>
- [17] Wang Y, Xiang F, Wang W, Wang WL, Su Y, Jiang F, Chen S, Riffat S (2020) Sound absorption characteristics of KGM-based aerogel. *Int J Low-Carbon Technol* 15:450–457. <https://doi.org/10.1093/ijlct/ctaa005>
- [18] Pu H, Ding X, Chen H, Dai R, Shan Z (2021) Functional aerogels with sound absorption and thermal insulation derived from semi-liquefied waste bamboo and gelatin. *Environ Technol Innovation* 24:101874. <https://doi.org/10.1016/j.eti.2021.101874>
- [19] Revin VV, Pestov NA, Shchankin MV, Mishkin VM, Platonov VI, Uglanov DA (2019) A study of the physical and mechanical properties of aerogels obtained from bacterial cellulose. *Biomacromol* 20:1401–1411. <https://doi.org/10.1021/acs.biomac.8b01816>
- [20] Cheng Z, Duan C, Zeng J, Wang B, Xu J, Gao W, Li J, Chen K (2021) Bottom-up ecofriendly strategy for construction of sustainable bacterial cellulose bioaerogel with multifunctional properties. *Adv Mater Interfaces* 8:2002101. <https://doi.org/10.1002/admi.202002101>
- [21] Chen W, Li Q, Wang Y, Yi X, Zeng J, Yu H, Liu Y, Li J (2014) Comparative study of aerogels obtained from differently prepared nanocellulose fibers. *Chemsuschem* 7:154–161. <https://doi.org/10.1002/cssc.201300950>
- [22] Fan B, Yao Q, Wang C, Jin C, Wang H, Xiong Y, Li S, Sun Q (2017) Natural cellulose nanofiber extracted from cell wall of bamboo leaf and its derived multifunctional aerogel. *Polym Compos* 39:3869–3876. <https://doi.org/10.1002/pc.24419>
- [23] NNT Thai QND Chau ND Do TD Tran HKP Huynh AT Nguyen XY Goh VTT Nguyen H Nguyen AN Phan ST Nguyen (2021) Fabrication of cellulose-based aerogel for thermal and acoustic insulation applications IOP Conf Ser: Earth Environ Sci 947 012030 <https://doi.org/10.1088/1755-1315/947/1/012030>
- [24] He C, Huang J, Li S, Meng K, Zhang L, Chen Z, Lai Y (2018) Mechanically resistant and sustainable cellulose-based composite aerogels with excellent flame retardant, sound-absorption, and superantwetting ability for advanced engineering materials. *ACS Sustainable Chem Eng* 6:927–936. <https://doi.org/10.1021/acssuschemeng.7b03281>
- [25] Hafez I, Tajvidi M (2021) Comprehensive insight into foams made of thermomechanical pulp fibers and cellulose nanofibrils via microwave radiation. *ACS Sustainable Chem Eng* 9:10113–10122. <https://doi.org/10.1021/acssuschemeng.1c01816>
- [26] Zhu G, Xu H, Dufresne A, Lin N (2018) High-adsorption, self-extinguishing, thermal and acoustic resistance aerogels based on organic and inorganic waste valorization from cellulose nanocrystals and red mud. *ACS Sustainable Chem Eng* 6:7168–7180. <https://doi.org/10.1021/acssuschemeng.8b01244>
- [27] Feng J, Le D, Nguyen ST, Nien VTC, Jewell D, Duong HM (2016) Silica–cellulose hybrid aerogels for thermal and acoustic insulation applications. *Colloid Surface A* 506:298–305. <https://doi.org/10.1016/j.colsurfa.2016.06.052>
- [28] Lefebvre J, Leblanc A, Genestie B, Chartier T, Lavie A (2016) Acoustic properties of aerogel encapsulated by macroporous cellulose. 23rd International Congress on Sound and Vibration. <https://www.researchgate.net/publication/306917581>
- [29] Silviana S, Hermawan F, Indrachya J, Kusumawardhani DAL, Dalanta F (2022) Optimizing the environmentally friendly silica-cellulose aerogel composite for acoustic insulation material derived from newspaper and geothermal solid waste using a central composite design. *J Sol-Gel Sci Technol* 103:226–243. <https://doi.org/10.1007/s10971-022-05831-y>
- [30] Pinto SC, Silva NHCS, Pinto RJB, Freire CSR, Duarte I, Vicente R, Vesenjajk M, Marques PAAP (2020) Multifunctional hybrid structures made of open-cell aluminum foam impregnated with cellulose/graphene nanocomposites. *Carbohydr Polym* 238:116197. <https://doi.org/10.1016/j.carbpo.2020.116197>
- [31] Shen L, Zhang H, Lei Y, Chen Y, Liang M, Zou H (2021) Hierarchical pore structure based on cellulose nanofiber/melamine composite foam with enhanced sound absorption performance. *Carbohydr Polym* 255:117405. <https://doi.org/10.1016/j.carbpol.2020.117405>
- [32] Cao L, Yu X, Yin X, Si Y, Yu J, Ding B (2021) Hierarchically maze-like structured nanofiber aerogels for effective low-frequency sound absorption. *J Colloid Interface Sci* 597:21–28. <https://doi.org/10.1016/j.jcis.2021.03.172>
- [33] Zhou S, Guo K, Bukhvalov D, Zhang XF, Zhu W, Yao J, He M (2020) Cellulose hydrogels by reversible ion-exchange as flexible pressure sensors. *Adv Mater Technol* 5:2000358. <https://doi.org/10.1002/admt.202000358>
- [34] Zhang XF, Ma X, Hou T, Guo K, Yin J, Wang Z, Shu L, He M, Yao J (2019) Inorganic salts induce thermally reversible and anti-freezing cellulose hydrogels. *Angew Chem Int Ed* 58:7366–7370. <https://doi.org/10.1002/anie.201902578>
- [35] Zhang X, Hou T, Chen J, Feng Y, Li B, Gu X, He M, Yao J (2018) Facilitated transport of CO₂ through the transparent and flexible cellulose membrane promoted by fixed-site carrier. *ACS Appl Mater Interfaces* 10:24930–24936. <https://doi.org/10.1021/acsami.8b07309>
- [36] Xu Q, Chen C, Rosswurm K, Yao T, Janaswamy S (2016) A facile route to prepare cellulose-based films. *Carbohydr*

- Polym 149:274–281. <https://doi.org/10.1016/j.carbpol.2016.04.114>
- [37] Rao AP, Rao AV, Pajonk GM (2007) Hydrophobic and physical properties of the ambient pressure dried silica aerogels with sodium silicate precursor using various surface modification agents. *Appl Surf Sci* 253:6032–6040. <https://doi.org/10.1016/j.apsusc.2006.12.117>
- [38] Guo H, Nguyen BN, McCorkle LS, Shonkwiler B, Meador MAB (2009) Elastic low density aerogels derived from bis[3-(triethoxysilyl)propyl]disulfide, tetramethylorthosilicate and vinyltrimethoxysilane via a two-step process. *J Mater Chem* 19:9054–9062. <https://doi.org/10.1039/B916355G>
- [39] Matias T, Varino C, Sousa HC, Braga MEM, Portugal A, Coelho JFJ, Durães L (2016) Novel flexible, hybrid aerogels with vinyl and methyltrimethoxysilane in the underlying silica structure. *J Mater Sci* 51:6781–6792. <https://doi.org/10.1007/s10853-016-9965-9>
- [40] Han T, Wang X, Xiong Y, Li J, Guo S, Chen G (2015) Lightweight poly(vinyl chloride)-based soundproofing composites with foam/film alternating multilayered structure. *Compos A* 78:27–34. <https://doi.org/10.1016/j.compositesa.2015.07.013>
- [41] Qin Q, Guo R, Ren E, Lai X, Cui C, Xiao H, Zhou M, Yao G, Jiang S, Lan J (2020) Waste cotton fabric/zinc borate composite aerogel with excellent flame retardancy. *ACS Sustain Chem Eng* 8:10335–10344. <https://doi.org/10.1021/acssuschemeng.0c00210>
- [42] Allard JF, Atalla N (2009) Propagation of sound in porous media: modelling sound absorbing materials, 2nd edn. Wiley, New York
- [43] Kuczmarski MA, Johnston JC (2011) Acoustic absorption in porous materials. NASA/TM-2011–216995. <https://ntrs.nasa.gov/citations/20110011143>
- [44] Soltani P, Taban E, Faridan M, Samaei SE, Amininasab S (2020) Experimental and computational investigation of sound absorption performance of sustainable porous material: Yucca Gloriosa fiber. *Appl Acoust* 157:106999. <https://doi.org/10.1016/j.apacoust.2019.106999>
- [45] Horoshenkov KV, Groby JP, Dazel O (2016) Asymptotic limits of some models for sound propagation in porous media and the assignment of the pore characteristic lengths. *J Acoust Soc Am* 139:2463–2474. <https://doi.org/10.1121/1.4947540>
- [46] Horoshenkov KV, Hurrell A, Groby JP (2019) A three-parameter analytical model for the acoustical properties of porous media. *J Acoust Soc Am* 145:2512–2517. <https://doi.org/10.1121/1.5098778>
- [47] Hu L, Zheng G, Yao J, Liu N, Weil B, Eskilsson M, Karabulut E, Ruan Z, Fan S, Bloking JT, McGehee MD, Wågberg L, Cui Y (2013) Transparent and conductive paper from nanocellulose fibers. *Energy Environ Sci* 6:513–518. <https://doi.org/10.1039/C2EE23635D>
- [48] Wu ZY, Li C, Liang HW, Chen JF, Yu SH (2013) Ultralight, flexible, and fire-resistant carbon nanofiber aerogels from bacterial cellulose. *Angew Chem* 125:2997–3001. <https://doi.org/10.1002/ange.201209676>

Publisher's Note Springer Nature remains neutral with regard to jurisdictional claims in published maps and institutional affiliations.

Springer Nature or its licensor (e.g. a society or other partner) holds exclusive rights to this article under a publishing agreement with the author(s) or other rightsholder(s); author self-archiving of the accepted manuscript version of this article is solely governed by the terms of such publishing agreement and applicable law.